Chapter 5

Graphene-based dual functional metadevice in the THz Gap

5.1 Introduction

The conventional MSs are limited by the functionalities as no structural modifications were allowed once they were designed, although a modern complex EM environment demands multifunctional features involving a single setup. A few literatures showed the way towards the dual functional performances of MSs by incorporating lumped elements (viz., PIN diode) to enable switching, such as absorber/reflector and absorber/rasorber etc. in the microwave regime [356]-[358]. The incorporation of the lumped elements in the MS design makes the structure lossy; thereby demanding the multifunctionality to meet out the current need of the EM applications. A few MS-based dual-functional devices in absorber/polarizer configuration were presented in the microwave bands [359]-[361], though their physical realizations seem to be difficult as all of them integrate lumped components to make the structural configurations bulky. The incorporation of the lumped components in the MS design provided dual functionality between absorption and cross polarization conversion of EM wave for narrowband applications in high frequencies [361]; however, the choice of materials for the design seems to be impractical.

A graphene-metal hybrid configuration without using any lumped components [359]-[361] has been introduced in this chapter to offer dual-functionality, i.e., absorption and cross-polarization conversion of EM wave. The ultrathin thickness and compactibility of the

Table 5.1. Comparison With Existing Dual-Functional Metadevices

Dual Functional Devices	Frequency range	Thickness	Periodicity	Configuration of the device	Angular Stability
1. [358] Dutta *et. al.*	15 GHz, 17 GHz	~λ_0/6.05	~λ_0/1.99	Metal-dielectric-metal-dielectric-metal (Lumped component used)	Not discussed
2. [359] Wang *et. al.*	2.56-7.62 GHz	~λ_0/11.15	~λ_0/4.88	Metal-dielectric-air spacer-metal (Lumped component used)	30°
3. [360] Li *et. al.*	3.7-10.7 GHz	~λ_0/9.13	~λ_0/4.05	Metal-dielectric-air spacer-metal (Lumped component used)	30°
Proposed Work	1-9 THz	~λ_0/12.49	~λ_0/5	Metal-dielectric-graphene-dielectric-metal (No lumped component used)	40°

proposed configuration in the THz gap have been improved by a factor of 1.12 and 1.02, respectively, than the microwave counterpart [360]. The dual-functional device (DFD) offers low-loss as it does not consist of any lumped components unlike [359]-[361]. It produces more than 70% absorptivity over a bandwidth of 3.40 THz together with a polarization conversion ratio (PCR) above 90% over a bandwidth of almost 3.87 THz (2.22 THz-6.09 THz) which is significantly improved compared to the gigahertz counterparts [359]-[361]. The metadevice operates in two different modes under the control of the external biasing. These findings are validated using a rigorous analysis of the equivalent circuit model followed by the derivation of the values of the circuit components using [298]. The proposed dual functional device is advantageous as it can operate for two different applications from the same configuration reducing the bulkiness of the system. It also improves the field confinement which can efficiently steer the THz signal [362]-[364]. The structural configuration of the proposed device is free from any lumped components which makes it less lossy. The device has ultrathin thickness and it is more compact obeying the effective homogeneity limit. The recent development in the dual functional devices has a great impact in our daily life in different ways, such as wearable and portable electronic devices, etc [365]. This type of device is on high demand for futuristic 6G communications and beyond as a variety of applications can be

realized by a single device in interference-free THz-gap. The proposed metadevice has been compared with the existing literatures as depicted in Table 5.1.

5.2 Configuration and Working Principle of the Device

The proposed metadevice is a five-layered structure. A specifically slot-patterned 1 nm thick The proposed metal-graphene hybrid metadevice has been analyzed electromagnetically by using CST Microwave Studio Suite [226]. It calculates the Maxwell's equations by using a numerical technique called finite integration technique (FIT). FIT has a versatile property

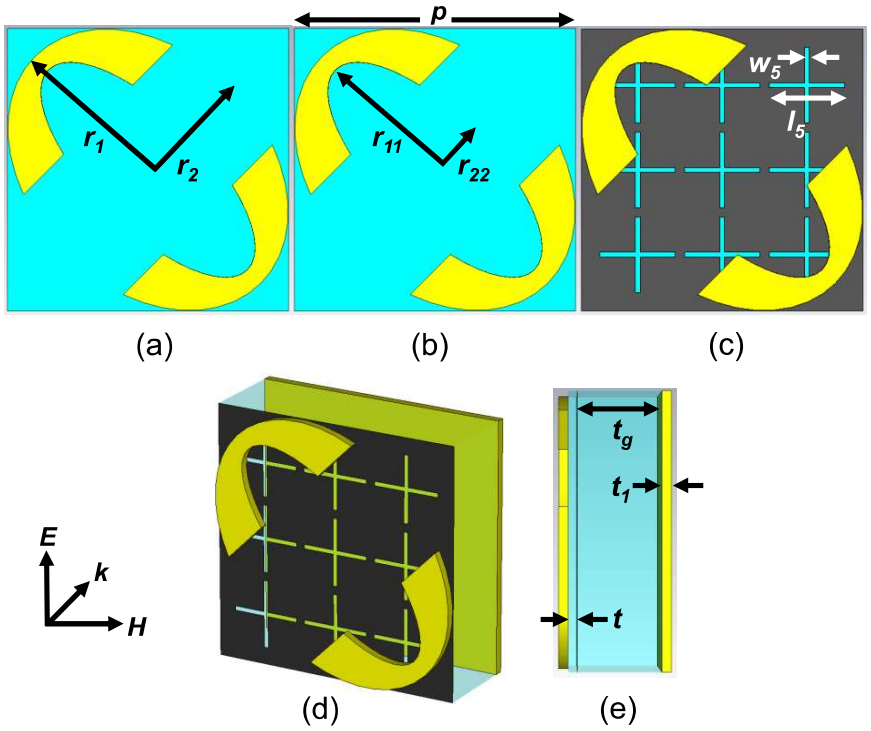

Fig. 5.1. (a, b, c) Top view, (d) perspective and (e) side view of the graphene-based dual-functional metadevice for absorption and cross-polarization conversion in THz-gap (r_1 = 17 µm, r_2 = 12.5 µm, r_{11} = 15 µm, r_{22} = 6 µm, p = 30 µm, w_5 = 0.5 µm, l_5 = 8 µm, t = 1 µm, t_1 = 1 µm, t_g = 9 µm).

which enables a problem to be calculated on a cartesian (hexahedral mesh) or non-orthogonal (tetrahedral mesh) grids in both time domain as well as in frequency domain. Tetrahedral shaped mesh cells have been used during electromagnetic simulations in frequency domain. In case of Mode I, 35,423 tetrahedral mesh cells have been used while in Mode II, 33,084 number

of tetrahedral mesh cells have been incorporated. The number of mesh cells is more in case of Mode I compared to Mode II as the patterned graphene metasurface acts as a metallic layer in Mode I (under the exposure of high value of the externally applied static electric field) whereas an insulating nature has been observed in Mode II. The device is analyzed using the infinite periodic boundary conditions imposed along the *xy*-plane and open boundary has been applied along the *z*-plane to allow the incidence of the plane EM wave. The unconventional electrical conductivity of graphene plays a major role in the spectral performances of absorber within the terahertz-gap (THz-gap) as it is a function of the applied electric field [366]-[367]. The periodically-patterned graphene metasurface deposited on the gold-backed thicker ZnO substrate (t_g) manipulates most of the incident linearly *y*-polarized (LP) EM wave to get absorbed into the structure. This particular configuration realizes a maximum absorptivity (A) of 90% at 6.84 THz within the desired spectral range under the exposure of an externally applied bias leading to a static electric field, ξ = 8.52 V/nm. The major radii (r_1 and r_2) and minor radii (r_{11} and r_{22}) of the two elliptical metallic split rings are designed in such a way that

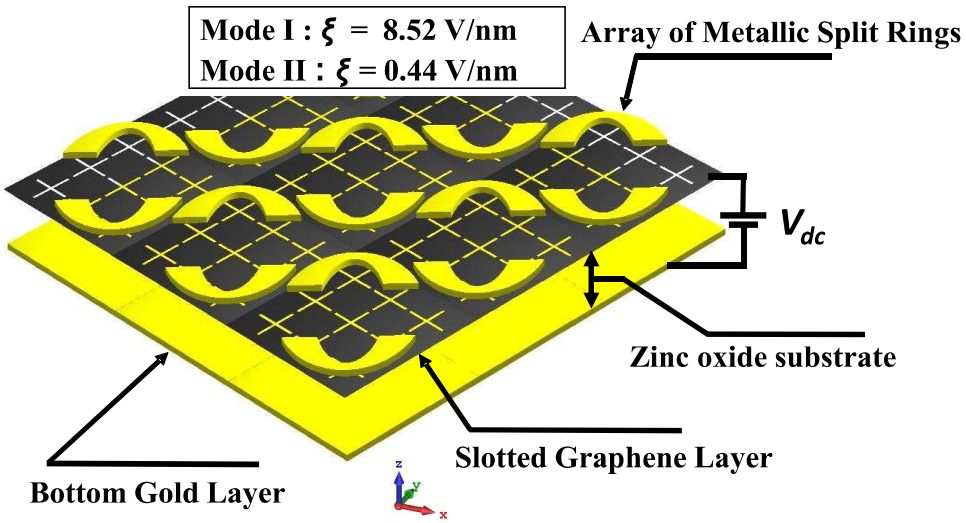

Fig. 5.2. Physical illustration of the biasing scheme of the proposed device with an external static electric field, ξ, applied between the patterned graphene surface and the bottom gold surface in periodic environment of the unit cell.

the *y*-polarized incident EM wave gets converted into the cross-polarized form achieving a maximum polarization conversion ratio (PCR) within the same frequency range while the value of ξ is changed to 0.44 V/nm. This set-up achieves near unity PCR peaks at 2.38 THz, 3.80 THz and 5.82 THz, respectively. A physical schematic of the biasing scheme of the proposed device has been presented in Fig. 5.2, where a variable DC voltage can be generated between graphene metasurface and the bottom gold surface by applying static electric filed externally [26].

5.3 Simulated Results and Discussions

The proposed metadevice offers two types of functionalities as discussed in the previous section. The optimized absorptivity performance of the device has been achieved when the patterned graphene metasurface is biased by an externally applied static electric field, ξ = 8.52 V/nm, indicated as Mode I in Fig. 5.3(a) while the maximum PCR has been achieved in Mode II when the static electric field has been switched to ξ = 0.44 V/nm as shown in Fig. 5.3(b). The change in electric field affects the Fermi level of the device which alters the chemical potential (μ_c); thereby modulating the surface conductivity [26].

During Mode I operation, the combination of the patterned graphene metasurface and the thicker ZnO layer backed by the continuous gold plate acts as an absorber (Abs), as depicted from Fig. 5.2. In this case, the conductivity of the patterned graphene layer becomes very high. In Mode II operation, the structural combination of the split-ring geometry together with the ZnO substrates backed by the continuous gold layer works as a cross-polarization converter as shown in Fig. 5.2. Here, the graphene layer acts as an insulator. The absorptivity performance (Abs) dominates over the PCR performance in Mode I as seen clearly in Fig. 5.3(a). On the contrary, the PCR performance dominates over the absorptivity performance (Abs) in Mode II as observed in Fig. 5.3(b). The absorptivity (A) has been calculated from equation (5.1), where

A stands for absorptivity, R is the reflection coefficient and T is the transmission coefficient produced by the proposed metadevice device in Mode I. The polarization conversion ratio

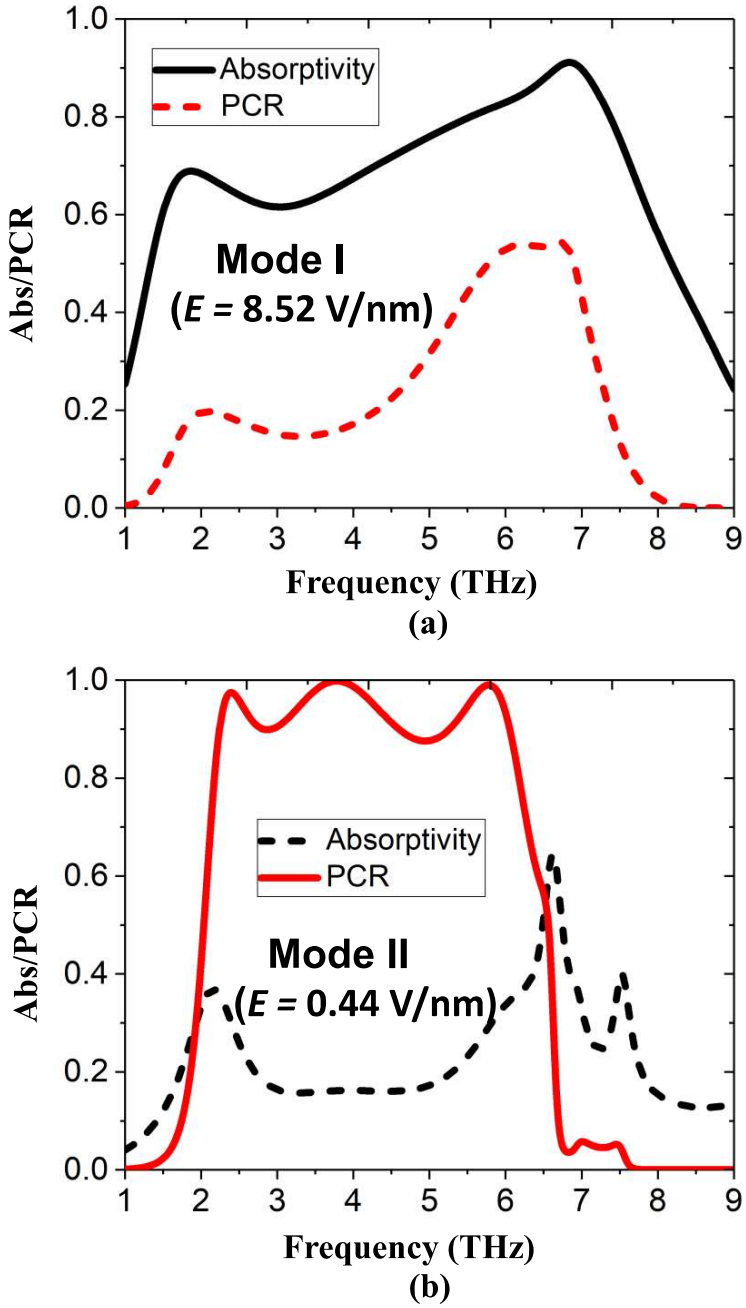

Fig. 5.3. (a). Optimized absorptivity performance of the proposed graphene-based dual-functional metadevice has been achieved when externally applied static electric field, $\xi = 8.52$ V/nm (Mode I) and (b). optimized PCR has been achieved at its maximum value when static electric field, $\xi = 0.44$ V/nm (Mode II).

(PCR), in Mode II, has been calculated from (5.2), where R_{yy} and R_{xy} are denoted as co- and cross-polarized reflection coefficients provided the incident EM wave is y-polarized.

$$A = 1 - |R|^2 - |T|^2 \qquad (5.1)$$

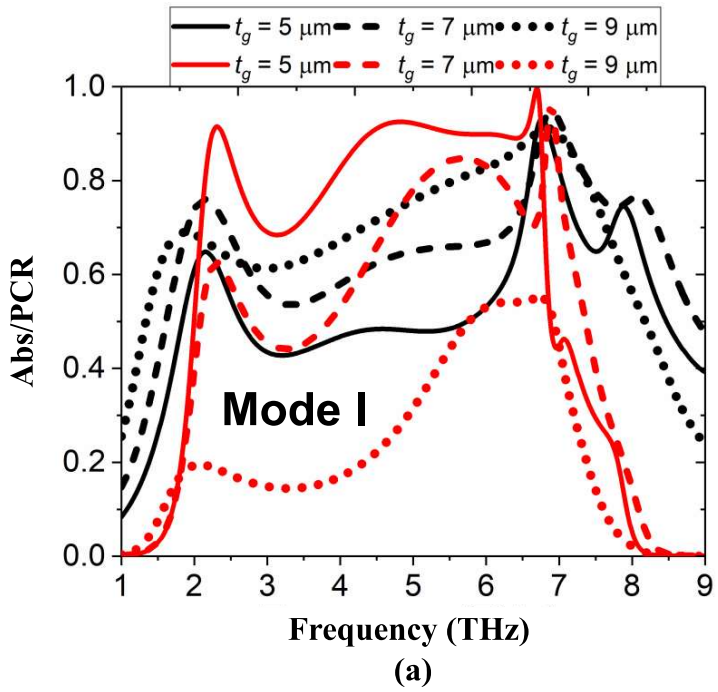

Fig. 5.4. Variation of the absorptivity (Abs) and cross-polarization conversion ratio (PCR) due to the change of the (a) height of the patterned graphene patch (t_g) from the ground gold surface and (b) size of the spatial span of the graphene patch (p_g) in Mode I operation of the device.

$$PCR = \frac{|R_{xy}|^2}{|R_{xy}|^2 + |R_{yy}|^2} \qquad (5.2)$$

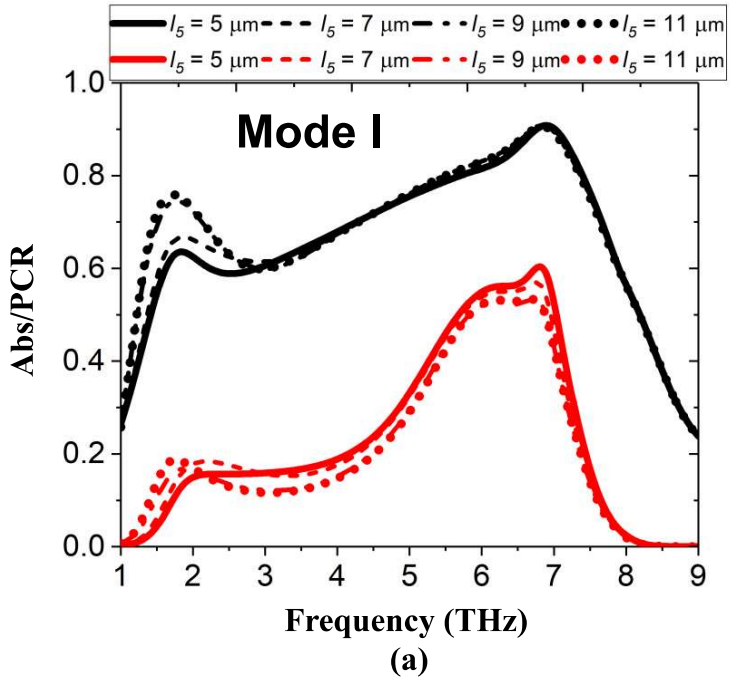

Fig. 5.5. Variation of the absorptivity (Abs) and cross-polarization conversion ratio (PCR) due to the change of the (a) length of the plus-shaped slots on graphene patch (l_5) and (b) width of the plus-shaped slots on graphene patch (w_5) in Mode I operation of the device. One can experience that the field-intensities are dense at the periodically arranged plus-shaped slot regions on the graphene surface while the metadevice is working in Mode I operation.

The proposed graphene-based device can achieve wideband dual functional performance of incident EM wave while changing the biasing scheme only, i.e., changing the DC bias voltage

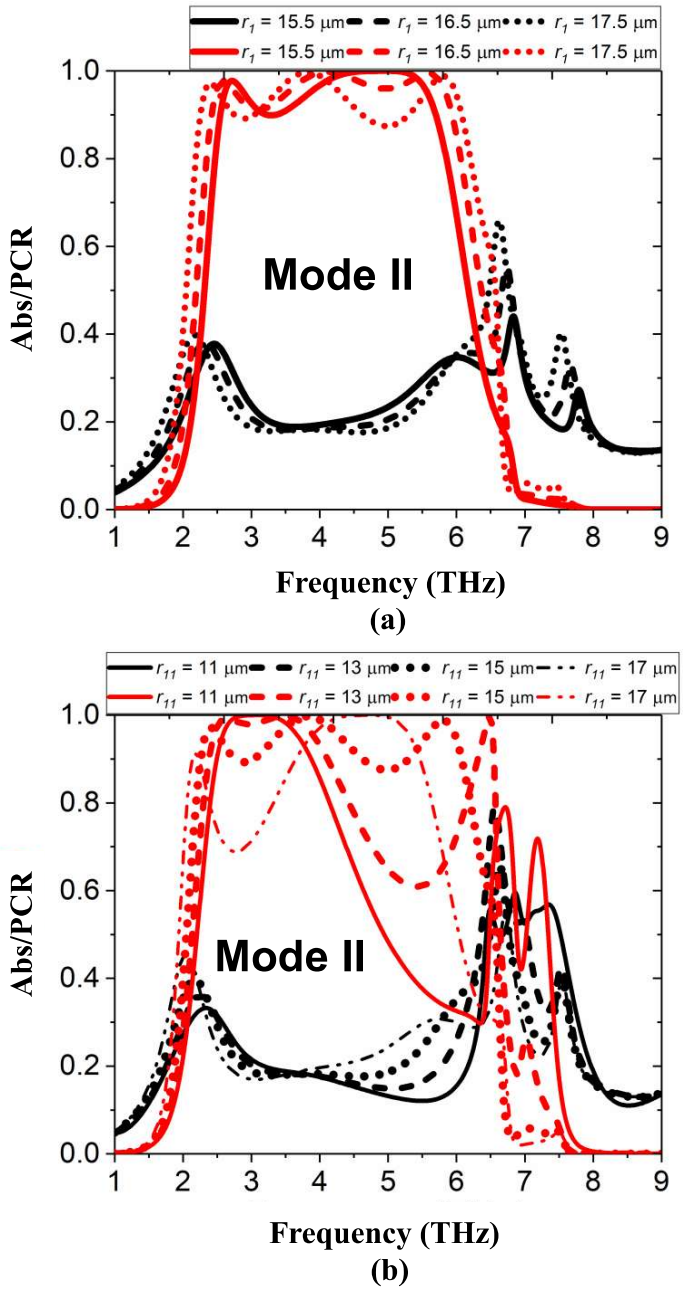

Fig. 5.6. Variation of the absorptivity (Abs) and cross-polarization conversion ratio (PCR) due to the change in the (a) outer major radii of the metallic split rings (r_1) and (b) inner major radii of the metallic split rings (r_{11}) in Mode II operation of the device.

V_{DC} induced by the applied static electric field, ξ, between the patterned graphene metasurface and the bottom gold layer as depicted in Fig. 5.2, without using any lumped components. The

optimized responses of the absorptivity (Abs) and PCR (cross-polarization conversion ratio) have been achieved after a rigorous study on the structural modifications of the device. The detailed study has been carried out by changing single structural parameter once at a time while

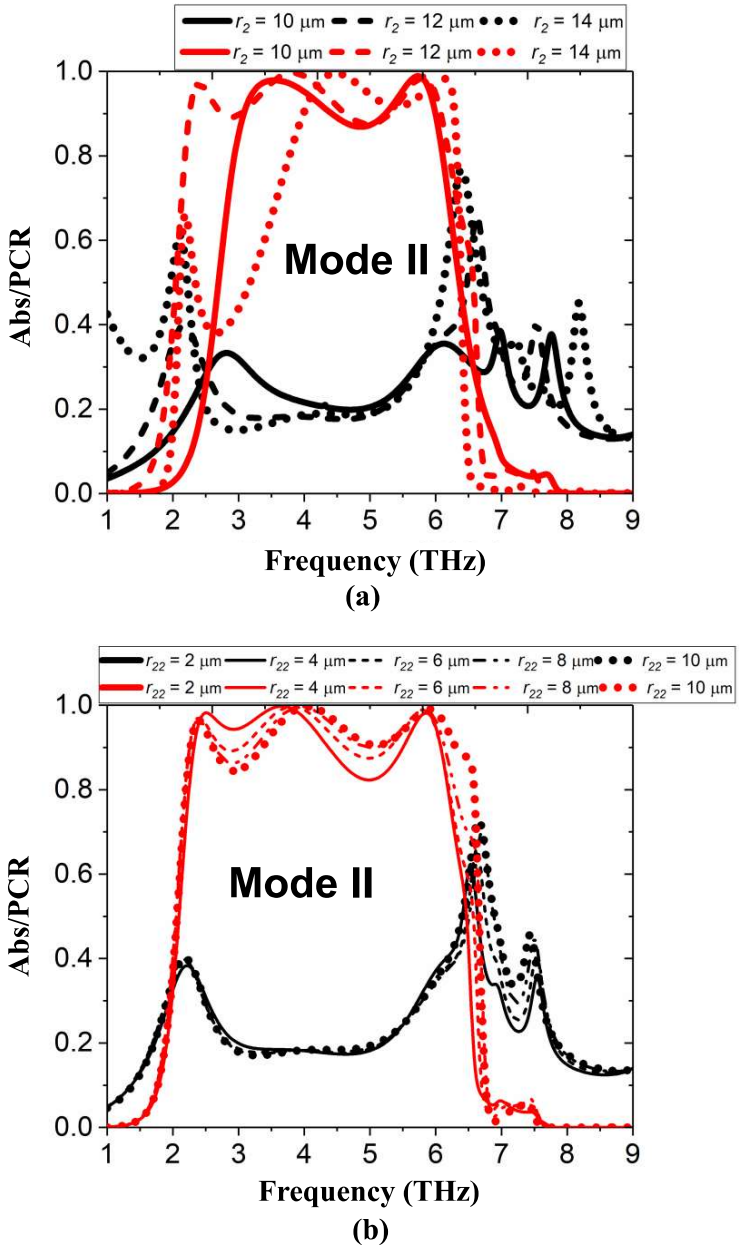

Fig. 5.7. Variation of the absorptivity (Abs) and cross-polarization conversion ratio (PCR) due to the change in the (a) outer minor radii of the metallic split rings (r_2) (b) inner minor radii of the metallic split rings (r_{22}) in Mode II operation of the device.

rest of the dimensions of the parameters remain invariant. First, the thickness (t_g) of the ZnO substrate holding the patterned graphene patch has been nurtured to check the best performance of the device. The coupling of the fields between the graphene metasurface and bottom gold layer is maximum when t_g = 9 μm in case of Mode I where the maximum absorption and minimum cross-polarization conversion of EM wave have been achieved as depicted from Fig. 5.4(a). The coupling between the spatially-spanned graphene metasurface and the bottom gold surface is also maximum in Mode I when the size of the graphene patch (p_g) is maximum, *i.e.*, p_g = 30 μm. Due to this, the device achieves maximum absorptivity (Abs) and minimum PCR over a broad bandwidth as shown in Fig. 5.4(b). The length and width of the plus shaped slots on the graphene surface are denoted as l_5 and w_5, respectively. These slots provide multiple resonances combined together within the spectral response [368]. The optimized absorptivity (Abs) has been achieved in Mode I operation of the metadevice when the length (l_5) of each arm of the plus-shaped slots is equal to 11 μm as verified from Fig. 5.5(a). The width (w_5) of each arm of the plus-shaped slots is set to 0.5 μm to provide an optimized absorptivity (Abs) response within the previously said spectral range as confirmed from Fig. 5.5(b). The above said fact can be validated by using the field-localization concept and can be illustrated in Fig. 5.12 [369].

Next, the structural modifications of the gold made split-ring geometry have been carried out to achieve the best cross-polarization conversion ratio (PCR) in Mode II operation of the metadevice. The outer and inner major radii of the elliptically-shaped metallic split rings are expressed as r_1 and r_{11} respectively. Similarly, the outer and inner minor radii of the above said split-ring geometry are termed as r_2 and r_{22} respectively. These dimensions are described in Fig. 5.1(a) and Fig. 5.1(b). The periodically-arranged elliptically-shaped metallic split-ring geometry is responsible for the conversion of the incident EM wave into its cross-polarized form

maximally when r_1 and r_{11} are stick to 17.5 µm and 15 µm respectively in Mode II operation of the device depicted in Fig. 5.6(a) and Fig. 5.6(b), respectively. Under the same condition, the device provides the best performance in terms of maximum PCR when r_2 and r_{22} are taken as 12 µm and 6 µm, respectively and they are plotted in Fig. 5.7(a) and Fig. 5.7(b), respectively. Next, the gap (w_3) between the two metallic split rings within the unit cell is examined for the optimized PCR performance in Mode II operation of the device. The best PCR performance with minimum absorption of EM wave has been realized for w_3 = 15.5 µm as one can verify from Fig. 5.8. The magnitude of co-polarized reflection coefficient (R_{yy}) is minimum while the magnitude of the cross-polarized reflection coefficient (R_{xy}) is maximum for w_3 = 15.5 µm, resulting into a maximum PCR. The periodicity (p) of the unit cell of the proposed device has been studied to select the best possible response of absorptivity (Abs) and polarization conversion ratio (PCR) during the incidence of EM wave on the proposed device. The most

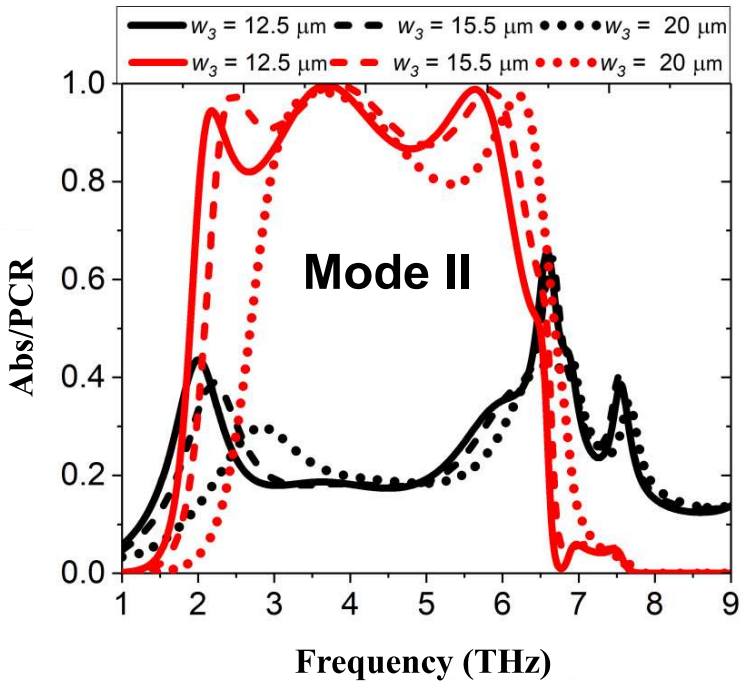

Fig. 5.8. Variation of the absorptivity (Abs) and polarization conversion ratio (PCR) due to the change in gap between the metallic split rings (w_3) within the unit cell in Mode II operation of the device.

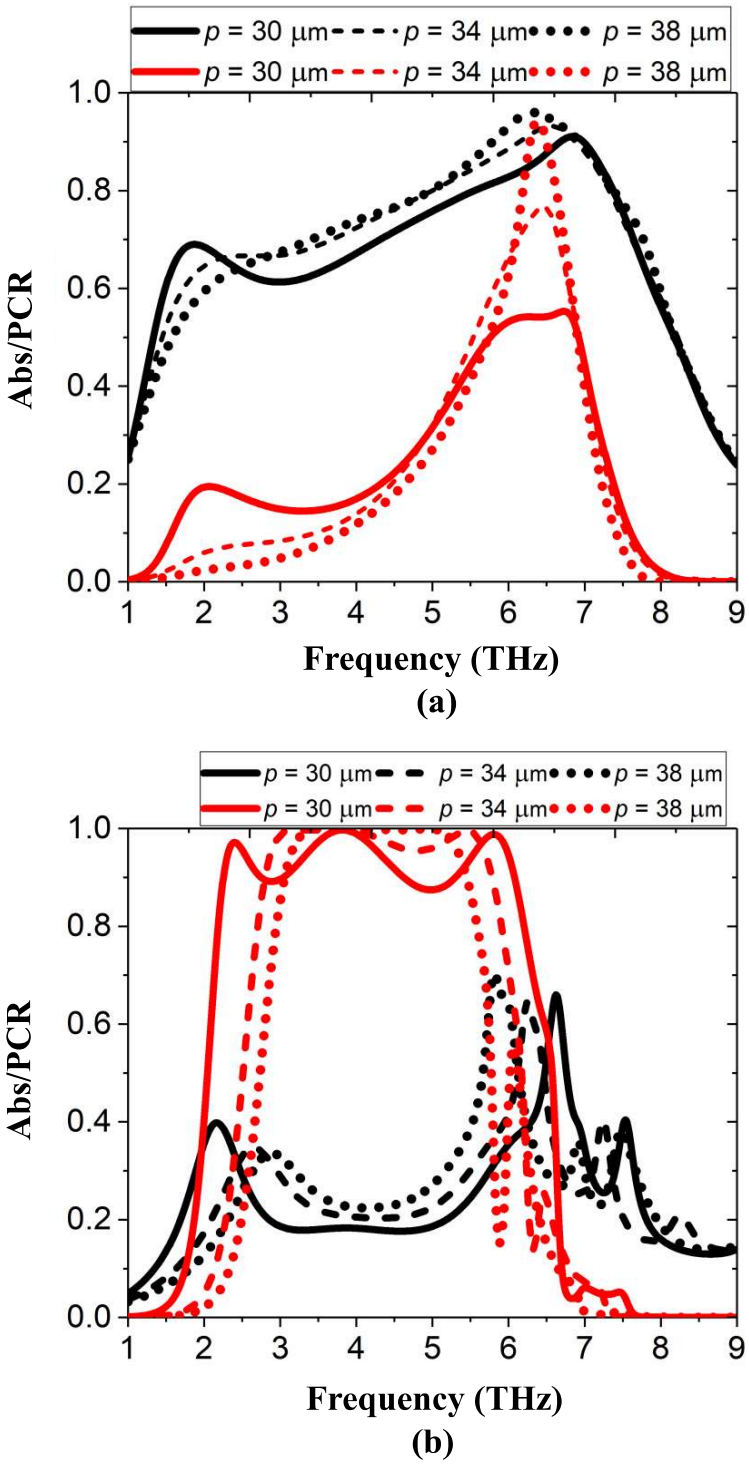

Fig. 5.9. Variation of the absorptivity (Abs) and polarization conversion ratio (PCR) due to the change in the periodicity (p) of the unit cell in (a) Mode I and (b) Mode II, operation of the device, respectively.

suitable absorptivity bandwidth has been achieved at p = 30 μm in Mode I as shown in Fig. 5.9(a). The best PCR bandwidth has also been achieved simultaneously at p = 30 μm in Mode II, as evident from Fig. 5.9(b). The proposed dual functional metadevice cannot be designed with two different periodicities at the same time within a single package. The proposed metadevice offers optimized performances of both absorption and cross-polarization conversion of the incident EM wave at a fixed periodicity value, *i.e.*, p = 30 μm; which further signifies the uniqueness of the proposed dual-functional metadevice. The proposed DFD has been compared to the existing designs in GHz domain as described in Table 5.1. It has advantages over thickness, periodicity, structural configurations and angular stability while in the exposure of the incident EM wave.

5.4 Circuit Realization

The EM simulated characteristics of the proposed dual-functional metadevice have been verified incorporating a circuit-model approach. The validity of both the absorption and cross-polarization conversion responses has been studied through the circuit model representation in Fig. 5.10 and Fig. 5.11, respectively. The circuit model simulations have been performed using the Keysight Advance Design System tool [298]. In Mode I operation of the device, the proposed structure acts as an absorber while the same device acts as a cross-polarization converter in Mode II. The respective schematics of the equivalent circuit models have been presented in Fig. 5.10 and Fig. 5.11. One can find the input impedance of the absorber configuration from the basic transmission line concept in Fig. 5.10(a) from (5.3) [339]

$$Z_1 = jZ_{t_g}\tan(kt_g)$$

$$Z_{in} = Z_1.Z_g/(Z_1 + Z_g)$$

$$Z_{in} = j(Z_g).Z_{t_g}\tan(kt_g)/(jZ_{t_g}\tan(kt_g) + Z_g) \qquad (5.3)$$

where Z_g stands for the surface impedance of the periodic graphene metasurface, Z_1 is the input impedance of the ZnO substrate, Z_{t_g} is the characteristics impedance of the ZnO substrate, t_g

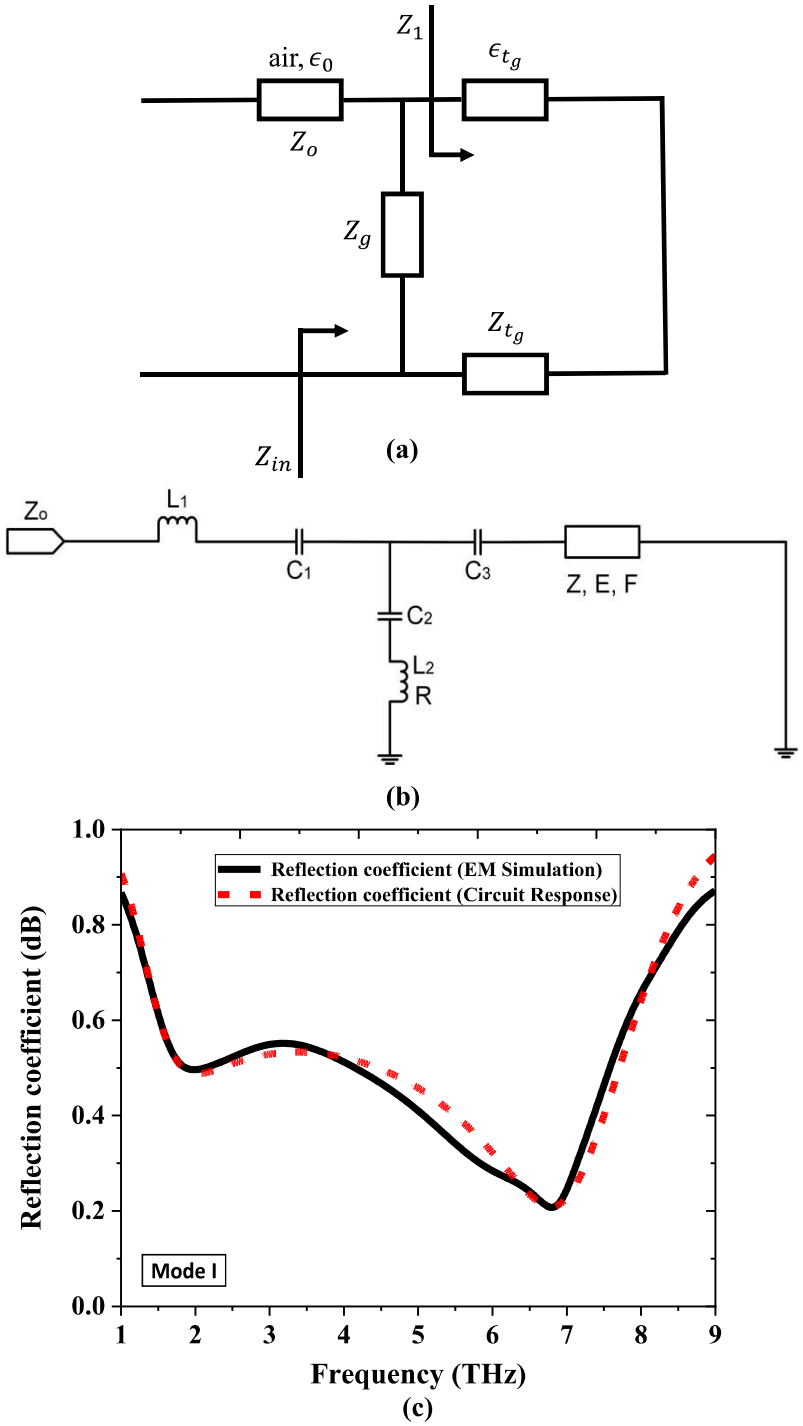

Fig. 5.10. Circuit schematics for the (a) absorber structure (Mode I), (b) an equivalent circuit model of the proposed metadevice working as an absorber and (c) the comparison of circuit model simulated response and EM simulated outcomes.

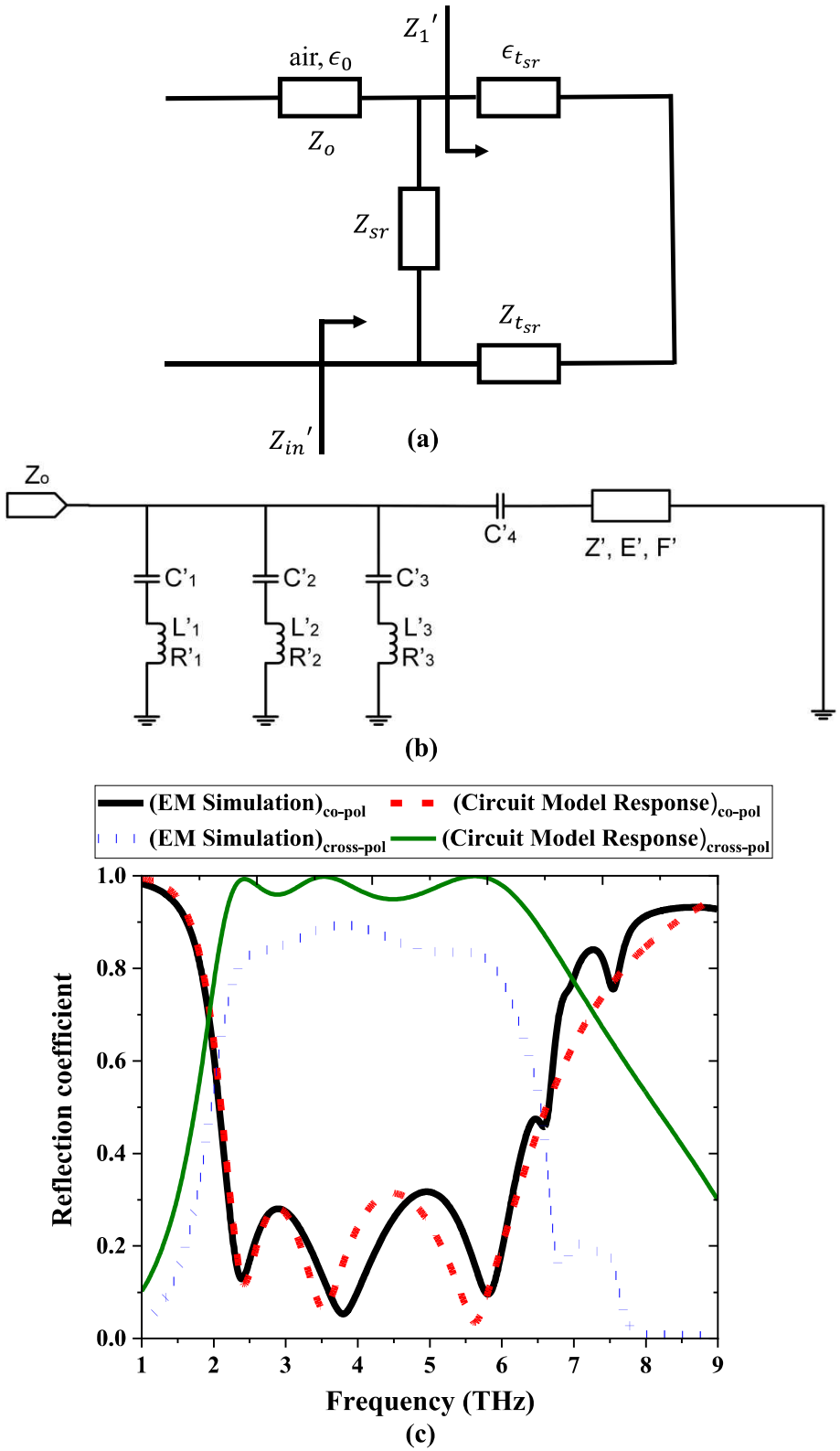

Fig. 5.11. Circuit schematics for the (a) cross-polarization converter structure (Mode II), (b) an equivalent circuit model for the proposed metadevice working as a cross-polarization converter and (c) the comparison of circuit model simulation and the EM simulation responses.

($t_g = 9$ µm) denotes the thickness of the ZnO substrate holding the graphene metasurface, ϵ_{t_g} is equal to the relative permittivity of the said substrate and k is the propagation constant of the electromagnetic wave within the said substrate. The reflection coefficient (Γ_{Abs}) for the absorber structure can be calculated as given in (5.4)

$$\Gamma_{Abs} = \left|\frac{Z_{in}-Z_o}{Z_{in}+Z_o}\right| \qquad (5.4)$$

The continuous graphene metasurface under the periodic boundary condition can be represented as a series combination of a capacitance (C_2), inductance (L_2) and a resistance (R) as the graphene patch exhibits dual nature of capacitive-inductive effect [293]. The periodically arranged plus-shaped slots are modeled as a LC circuit component (L_1 and C_1) connected in parallel to the previously said RLC circuit combination. The surface impedance (Z_g) can be calculated from these circuit components as shown in Fig. 5.10(b). The ZnO substrate has been considered as a transmission line as a function of Z, E and F, where Z = Z_{t_g}, E = phase and F = one of the frequency instances within the operating band as the substrate can change the phase of the EM wave. A capacitance (C_3) has been introduced to consider the coupling between the graphene metasurface and the bottom gold surface. The other end of the transmission line has been connected to the ground because of the bottom metallic plane. The above said details have been described as Fig. 5.10(b).

Similarly, the input impedance for the polarization converter structure can be found from Fig. 5.11(a) as seen from (5.5)

$$Z_{in}{}' = j(Z_{sr}).Z_{t_{sr}}{}' \tan(k't_{sr})/(jZ_{t_{sr}}{}' \tan(k't_{sr}) + Z_{sr}) \qquad (5.5)$$

where Z_{sr} stands for the surface impedance of the periodic split-ring metasurface, $Z_1{}'$ is the input impedance of the ZnO substrate of the cross-polarization converter configuration, $Z_{t_{sr}}$ is the characteristic impedance of the ZnO substrate of the cross-polarization converter structure, t_{sr} ($t_{sr} = (t_g + t) = 10$ µm) denotes the thickness of the ZnO substrate holding the split-ring

metasurface, $\epsilon_{t_{sr}}$ is equal to the relative permittivity of the said substrate ($\epsilon_{t_g} = \epsilon_{t_{sr}}$, as the substrate are same in Mode I and Mode II) and k' is the propagation constant of the electromagnetic wave within the said substrate. The co- polarized reflection coefficient $(\Gamma_{Abs}{}')_{co}$ can be found by equation (5.6),

$$(\Gamma_{Abs}{}')_{co} = \left|\frac{Z_{in}{}'-Z_o}{Z_{in}{}'+Z_o}\right| \qquad (5.6)$$

The cross-polarized reflection coefficient can be found from equation (5.7),

$$(\Gamma_{Abs}{}')_{cross} = [1 - |(\Gamma_{Abs}{}')_{co}|^2]^{\frac{1}{2}} \qquad (5.7)$$

The periodically arranged split-ring resonators have been modeled as a cascaded parallel configuration of three RLC circuit components (C'$_1$, L'$_1$, R'$_1$; C'$_2$, L'$_2$, R'$_2$; and C'$_3$, L'$_3$, R'$_3$, respectively) as shown in Fig. 5.11(b). The surface impedance (Z_{sr}) of this metallic metasurface can be calculated from these distributed circuit components. They all are connected to a coupling capacitance, C'$_4$, in between the bottom gold surface and the top metallic split-ring metasurface. The ZnO substrate has been modeled as a transmission line as shown in Fig. 5.11(b).

The absorptivity and PCR has been calculated using the co- and cross-polarized reflection coefficients (R_{yy} and R_{xy}) extracted from the EM simulation of the device. The optimized values of the circuit components for Mode I and Mode II operation of the device are presented in Table 5.2. The R_{yy} and R_{xy} responses have also been derived from the proposed equivalent circuit-model of the metadevice operated in Mode I and Mode II as illustrated in Fig. 5.10(c) and Fig. 5.11(c), respectively. It can be concluded that the EM simulated responses and circuit simulation results are in excellent resemblance in terms of co-polarized reflection coefficient. There is a negligible difference between the cross-polarized reflection coefficients generated from the EM simulation as well as the circuit model approach. This may be because of the fact that the loss in the overall structure has not been considered in the circuit model approach [370].

5.5 Discussions

The wave-matter interaction has been demonstrated in terms of electric field distribution [magneto-plasmonic case] at 3.8 THz in Fig. 5.12(a). Under the exposure of the EM wave, the electric field is more concentrated on the device in Mode I as the biased graphene pattern interacts more with the EM wave in terms of interactions between electrons and EM wave. The electric field is less concentrated in Mode II at 3.8 THz as the patterned graphene surface acts as an insulator in this condition (ξ = 0.44 V/nm) and the incident EM wave mostly interacts with the metallic split-rings. The field distribution responses have been shown for unit cell of the device, as confirmed from Fig. 5.12. Electric field localization, an essential need for nanophotonics, has been formed very efficiently in case of Mode I as graphene supports surface plasmon polaritons (SPPs) and localized surface plasmon polaritons (LSPPs) very efficiently. Under the exposure of the incident EM wave, the electrons of the metallic split-rings together

Table. 5.2. Optimized Values of the Circuit Components

Proposed Metadevice [Mode I] (RLC Components)	**Optimized Values for the RLC Components [Mode I]**	**Proposed Metadevice [Mode II] (RLC Components)**	**Optimized Values for the RLC Components [Mode II]**
C_1	1.2 pF	C'_1	0.0642 fF
C_2	0.5117 fF	C'_2	0.0535 fF
C_3	169.9646 fF	C'_3	0.0642 fF
L_1	5×10^{-5} nH	C'_4	120.1012 fF
L_2	7.16 pH	L'_1	0.1 pH
R	172.316 Ω	L'_2	21.793 pH
Z	264 Ω	L'_3	55.483 pH
E	90°	R'_1	120 Ω
F	5 THz	R'_2	235.3 Ω
		R'_3	319.7 Ω
		Z'	264 Ω
		E'	90.1°
		F'	5 THz

with the patterned graphene surface gets polarized and generates field localizations [371]. The plus-shaped periodic slots on the graphene surface cause the field localization due to the localized surface plasmonic resonances (LSPR) at 3.8 THz as shown in Fig. 5.12. The surface current distributions of the top and bottom layers have been described in two different modes at 3.8 THz as provided in Fig. 5.13. The surface currents of the top and bottom layers of the device

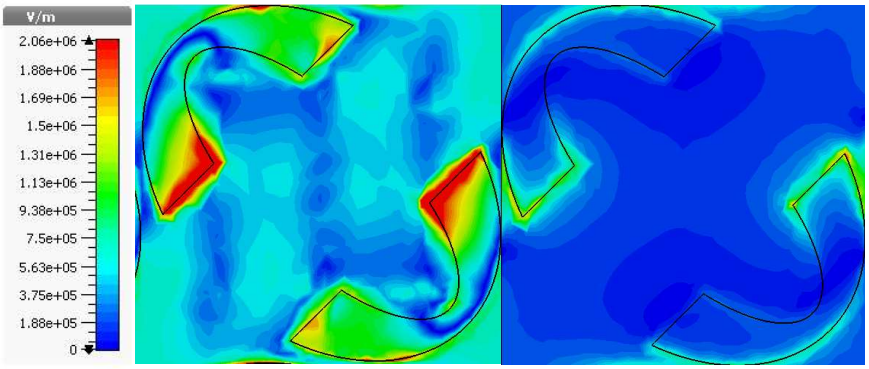

(a) Field concentration on the unit cell at 3.8 THz

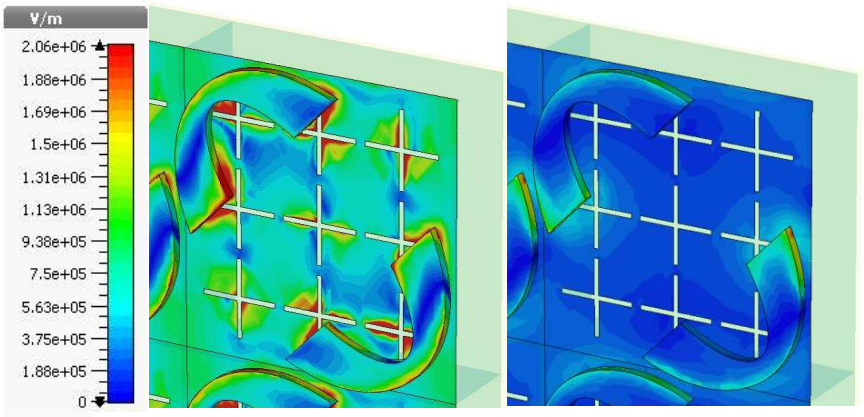

(b) Perspective view of the field concentration on the unit cell at 3.8 THz

Fig. 5.12. (a) Field concentration on the unit cell of the proposed device under two different conditions in Mode I and Mode II at 3.8 THz (Magneto-plasmonic case).

are antiparallel in nature indicating the magnetic resonance at 3.8 THz. The intensity and density of the surface currents are much larger in Mode I compared to that of Mode II, as revealed from Fig. 5.13. This may be because of the fact that the graphene pattern acts as a

metallic layer in Mode I for a high chemical potential value induced by the static electric field (ξ) applied externally; which further adds up more conductivity on the graphene surface of the device than that of the Mode II where graphene layer is acting as an insulator without adding up any additional conductivity into it.

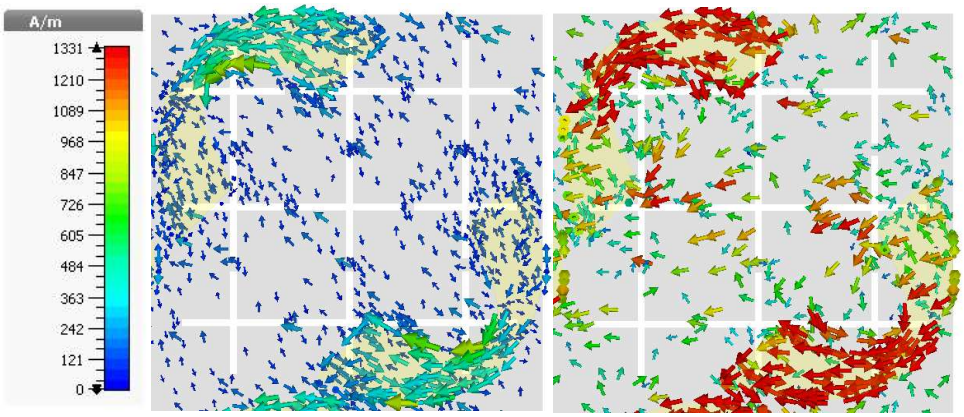

Fig. 5.13. Surface current distributions on both (a) top and (b) bottom surfaces under two different conditions in Mode I and Mode II at 3.8 THz.

5.6 Conclusions

A multilayered device with a combination of metal-dielectric-graphene-dielectric-metal layers, has been demonstrated to provide a dual functional performance of absorption and cross-polarization conversion in the THz gap while it interacts with the EM wave. The device offers more than 70% absorptivity over a bandwidth of 3.40 THz (between 4.25 THz and 7.65 THz)

with a 90% absorptivity peak at 6.84 THz under the static electric field of ξ = 8.52 V/nm. The device can also produce a PCR more than 90% over a bandwidth of 3.87 THz (between 2.22 THz - 6.09 THz) with near unity PCR peaks at 2.38 THz, 3.80 THz and 5.82 THz respectively at ξ = 0.44 V/nm. The device is very promising for futuristic applications as it performs dual functionality from a single physical configuration without the integration of lumped components. The structure has also been analyzed in the light of equivalent circuit-model. The circuit model responses in the two modes are found to be in good resemblance with the respective EM simulated responses. The device finds potential applications for THz detection, THz communication, THz imaging, THz sensing, wearable and portable electronic devices, 5G/6G communications and beyond.